by boron and aluminum atoms. The structure offers a good chance for substitution of aluminum [and the boron atoms in 8(*f*)] by other ions or atoms over a wide range.

The two-dimensional analysis was performed while the author was a staff member of the U.S. Army Electronics Research and Development Laboratory, Fort Monmouth, New Jersey, U.S.A. It is a pleasure to acknowledge the continuing interest and many profitable discussions during that time with Dr J. A. Kohn, who also kindly provided the crystal. The three-dimensional work was done at the Eduard Zintl Institut, Technische Hochschule, Darmstadt, and it is my special privilege to thank Prof. Wölfel for his interest and encouragement. I am further indebted to Mrs H. Gross for the densitometer measurements, and the Deutsches Rechenzentrum and the Rechenzentrum der Technischen Hochschule Darmstadt for providing computer time.

References

CLARK, H. K. & HOARD, J. L. (1943). *J. Amer. Chem. Soc.* **65**, 2115.
DECKER, B. F. & KASPER, J. S. (1959). *Acta Cryst.* **12**, 503.
ERIKS, C. (1961). Private communication.
HOARD, J. L., HUGHES, R. E. & SANDS, D. E. (1958). *J. Amer. Chem. Soc.* **80**, 4507.
HOPPE, W. (1957). *Z. Elektrochem.* **61**, 1076.
HOPPE, W. & WILL, G. (1960). *Z. Kristallogr.* **113**, 104.
HUGHES, R. E., KENNARD, C. H. L., SULLENGER, D. B., WEAKLIEM, H. A., SANDS, D. E. & HOARD, J. L. (1963). *J. Amer. Chem. Soc.* **85**, 361.
KOHN, J. A., KATZ, G. & GIARDINI, A. A. (1958). *Z. Kristallogr.* **111**, 53.
LIPSCOMB, W. N. & BRITTON, D. (1960). *J. Chem. Phys.* **33**, 275.
LONGUET-HIGGINS, H. C. & ROBERTS, M. DE V. (1955). *Proc. Roy. Soc.* A, **230**, 110.
WILL, G. (1963*a*). *Z. Kristallogr.* **119**, 1.
WILL, G. (1963*b*). *J. Amer. Chem. Soc.* **85**, 2335.
WILL, G. (1964). USAELRDL Technical Report 2436.

Acta Cryst. (1967). **23**, 1079

The Crystal Structure of Dimanganese Iron Carbonyl, $Mn_2Fe(CO)_{14}$*

BY P. A. AGRON, R. D. ELLISON AND H. A. LEVY

Chemistry Division, Oak Ridge National Laboratory, Oak Ridge, Tennessee, U.S.A.

(*Received* 28 *April* 1967)

X-ray peak-top data were collected with a computer-controlled diffractometer programmed to optimize precision by adjusting peak and background counting times and to reject weak reflections. The structure was solved by inspection of the Patterson diagram. The structure contains two crystallographically distinct molecules of symmetry 2/*m*. The iron atoms are situated at the non-equivalent symmetry centers 000 and $0\frac{1}{2}\frac{1}{2}$ of the monoclinic unit cell ($C2/m$, $a=11{\cdot}94$, $b=14{\cdot}29$, $c=11{\cdot}73$ Å, $\beta=97{\cdot}23°$, $Z=4$). Both molecules have linear arrangements of metal atoms, without bridging carbonyl linkages. Each metal atom is essentially octahedral, with the carbonyl ligands on Mn oriented at 45° to those on Fe. The molecules differ in disposition of symmetry elements: in one, three metal atoms, two carbonyl ligands of Fe, and the apical ligands of Mn lie in the mirror, with the remaining ligands of Fe along the diad; in the other, the metal atoms and the apical ligands lie along the diad, with the remaining 4 ligands of Fe in the mirror. Interatomic distances are Fe–Mn, 2·80–2·83; Fe–C, 1·79–1·80; Mn–C (apical), 1·80–1·82; Mn–C (equatorial), 1·85–1·86; C–O, 1·12–1·15 Å.

Bonding between the metal atoms in polynuclear metal carbonyls is of two kinds. In some compounds the carbonyl group forms a bridge, as in $Fe_2(CO)_9$ (Powell & Ewens, 1939); in other cases the metal atoms are directly linked, as in $Mn_2(CO)_{10}$ (Dahl & Rundle, 1963; Bailey & Dahl, 1965) and its rhenium and technetium analogues. Compounds with bridging carbonyl groups show a characteristic infrared absorption band at about 1850 cm^{-1}.

A trinuclear carbonyl identified as $Mn_2Fe(CO)_{14}$ has been prepared by Schubert & Sheline (1965) by the photolysis with ultraviolet light of an equimolar solution of $Fe(CO)_5$ and $Mn_2(CO)_{10}$ in n-hexane. In the spectrum of this compound there is no band in the neighborhood of 1850 cm^{-1} (private communication); thus it appeared likely that the molecule had the structure $(CO)_5MnFe(CO)_4Mn(CO)_5$ without bridging CO groups. The present study confirms this hypothesis and establishes the molecular configuration and dimensions.

Experimental

A sample of the red, needle-shaped crystals was furnished by Professor Sheline and Dr George Evans of Florida State University. The specimen selected for

* Research sponsored by the U.S. Atomic Energy Commission under contract with the Union Carbide Corporation.

study was a short pillar, $0{\cdot}15\times0{\cdot}20\times0{\cdot}32$ mm, with irregular ends.

Precession photography with Mo $K\alpha$ radiation showed the space group to be $C2/m$, $C2$, or Cm (reflections hkl were absent for $h+k$ odd). The diffractometer angles of eight reflections in the 2θ-range 39 to 49° were measured (Mo $K\alpha_1$, $\lambda=0{\cdot}70926$ Å) to determine the unit-cell parameters and the orientational coordinates of the specimen. Adjustment by the method of least-squares yielded

$$a=11{\cdot}935,\ b=14{\cdot}287,\ c=11{\cdot}732\ \text{Å},\ \beta=97{\cdot}23°$$

(least squares standard deviations 0·004 Å and 0·02°). The calculated density for 4 molecules per unit cell is 1·866 g.cm^{-3}, in good agreement with the measured value 1·867 (Evans, Hargaden & Sheline, 1967).

This study was undertaken as an exercise in rapid structure determination, making full use of the capability of the Oak Ridge Computer-Controlled Diffractometer (Busing, Ellison, Levy, King & Roseberry, 1967) to optimize the precision of the data by adjusting the parameters of the measuring process. The stationary-crystal, stationary-counter method with niobium-filtered Mo $K\alpha$ radiation was employed. The time to be devoted to a given reflection was chosen to achieve a standard deviation in the net count of 5%. Counting to a given relative standard error is suggested by our experience in other structure determinations that the accuracy of the best-determined intensities is unlikely to be greater than some relative minimum, usually about 3%, regardless of the statistical precision achieved. For a given total time T to be spent on a reflection, there is an optimal division between peak and background counting times, t_p and t_b respectively, which minimizes the error in the net count:

$$(t_p/t_b)^2=r_p/r_b\,,\quad t_p+t_b=T\,, \tag{1}$$

in which r_p and r_b are the peak and background counting rates (see for example Mack & Spielberg, 1958). With this division of time, the total time required for a given expectation of the relative error $S=\sigma(n)/n$, $n\equiv r_p-r_b$, is

$$T=[(r_p^{1/2}+r_p^{1/2})/nS]^2 \tag{2}$$

(Mack & Spielberg, 1958). In the procedure adopted, the peak and background rates were first estimated by two-second sampling counts, and the total time T was computed. If this time exceeded two minutes, as was the case for the weakest peaks, the reflection was not further measured, since the weak reflections were judged not to contribute substantially to the solution of the structure.

If the stationary-crystal method is to yield integrated intensities, the source must irradiate the sample with uniform intensity over a range of incident angle greater than the combined mosaic distribution and spectral width. The intensity profile of the source at 10° take-off angle, shown in Fig. 1, was estimated by θ–θ scanning (the detector and crystal displaced by the same angular increments) of a low-angle reflection ($2\theta=7{\cdot}3°$) with a narrow counter aperture. Pinhole photographs of the focal spot indicated that the source subtends about 0·56° at the sample, in fair agreement with Fig. 1. The full mosaic width of the specimen (at about 3% of maximum) was estimated by ω-scanning several reflections at low angles (with small take-off angle and narrow counter aperture) to be 0·14°; the portion of the intensity profile required to integrate over this mosaic width and the Mo $K\alpha$ doublet, at various 2θ values, is shown by the solid lines in the Figure. Clearly, the conditions are far from ideal. Errors will arise both from the lack of a truly uniform central portion and, at the largest Bragg angles, from reduced intensity incident on the tails of the mosaic distribution. Fortunately the tails contribute relatively little to the integrated intensity. In order to evaluate these errors, a comparison was made for several reflections of stationary-crystal measurements with moving crystal (θ–2θ scan) measurements (see Fig. 2). We concluded that the stationary-crystal measurements are valid to a scattering angle 2θ of 35° and that between 35 and 50° the stationary crystal measurements require correction by a factor estimated as

$$C=1+6{\cdot}47[(\sin\theta/\lambda)-0{\cdot}423]^2\,,$$

shown by the solid line in Fig. 2; in this range, the scatter is larger also. For the purpose of refinement

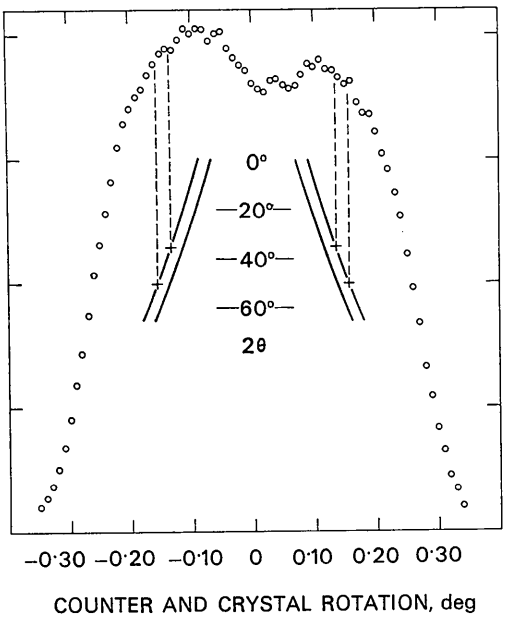

Fig. 1. The intensity profile of the X-ray source as measured by a θ–θ scan of a low-angle Bragg reflection with narrow counter aperture. The abscissa is the rotation angle of counter and crystal (equal to the 2θ-coordinate change and to twice the ω-coordinate change). The solid lines indicate the portion of the profile required to integrate a reflection from the $Mn_2Fe(CO)_{14}$ specimen at various values of 2θ. The inner pair applies to the stationary specimen; the outer pair to the pseudo-stationary measurement (2-step 2θ-scan) used in this study. The dotted lines indicate the requirements at 35° and 50° 2θ.

by the method of least squares, we estimated the variance of an observation to be

$$V_{\text{statistical}} + (0{\cdot}04F_o^2)^2 , \qquad 2\theta \leq 35^\circ$$

or

$$V_{\text{statistical}} + F_o^2 C^2 [0{\cdot}04 + 0{\cdot}754(\sin\theta/\lambda - 0{\cdot}423)]^2 , \qquad 2\theta > 35^\circ .$$

The corresponding standard errors are indicated by dotted lines in Fig. 2.

The time for counting background was divided between two settings, one with the 2θ coordinate of the diffractometer set at 1° below the computed value and the other with it 1° above. The time for counting the peak was divided among 3 settings 0·04° apart in 2θ. This pseudo-stationary measurement sampled the 'flat' top of the diffraction peak at 3 neighboring points; it was intended to even out fine-scale non-uniformity in the source intensity. Each count was corrected for amplifier dead time (3·8 microseconds); the net rate and its statistical standard deviation were computed and punched on the output paper tape of the controlling computer.

From 1807 symmetrically non-equivalent reflections examined, this procedure yielded measurements for 802 reflections that were strong enough to satisfy the selection criterion. A reference reflection was measured about once per hour and used to correct for slow variations in the incident beam power. Since the sampling of the counting rates, on which the selection of reflections depended, was itself subject to statistical error, it is not expected that there should be a sharp intensity difference between measured and unmeasured reflections. The distribution that resulted from our procedure is shown in Fig. 3, in which the frequency of occurrence of reflections in both groups is plotted against the calculated intensity for the final refined model.

The integrated intensities were corrected for absorption by a computation in which the specimen shape was approximated as an ellipsoid. The linear absorption coefficient is 21·3 cm^{-1}; the resulting transmission factors range between 0·71 and 0·78. A Wilson analysis of the squared structure-factors, in which zero values were ascribed to all unobserved reflections, yielded an approximate absolute scale, an over-all temperature factor coefficient $B = 5{\cdot}3$ Å^2, and a set of normalized structure factor magnitudes $|E_h|$.

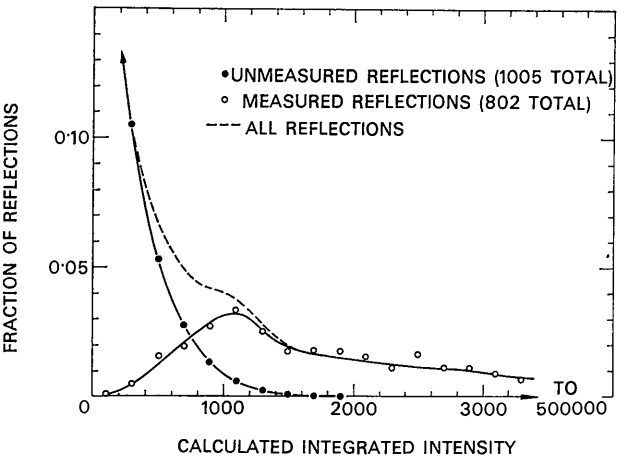

Fig. 3. The distribution of measured and unmeasured reflections as a function of calculated integrated intensity, $F^2(1+\cos^2 2\theta)/(2\sin 2\theta)$. The minimum value of Q for which 5% statistical standard error is expected in a two-minute count is approximately 690. Statistical fluctuations in the two-second sampling counts produce the tailing of the two distributions above and below this value.

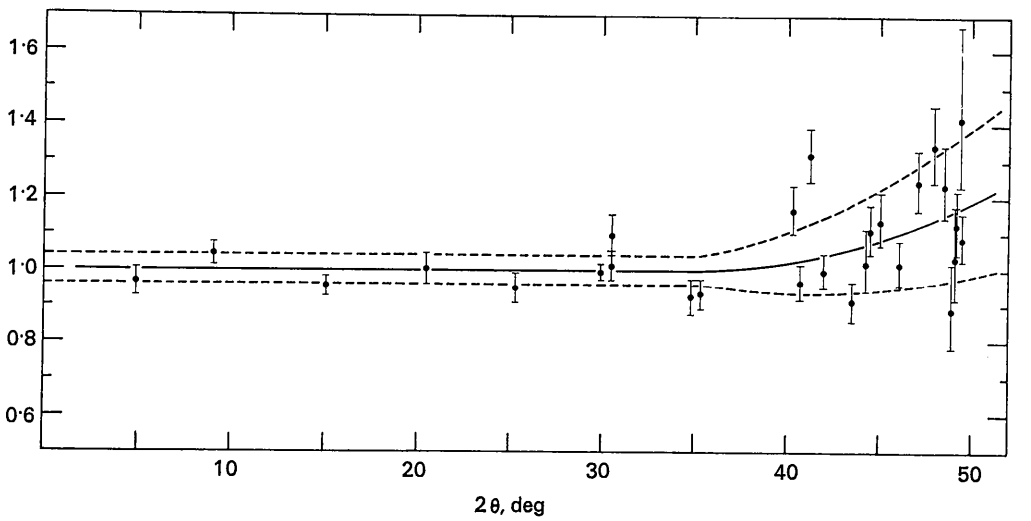

Fig. 2. The normalized ratio of integrated intensities measured by 2θ-scanning to those measured with a stationary crystal. The solid line indicates the correction factor adopted; the dotted lines indicate the estimated standard deviation in this factor, used to establish weights for refinement by the least-squares method. The short vertical lines represent the standard deviations of the points.

Table 1. *Calculated and observed structure amplitudes for* $Mn_2Fe(CO)_{14}$

The columns contain, respectively, the Miller index l, calculated F, observed F magnitude, and error in $|F|$ computed as $\sigma(F^2)/2F$. Miller indices h and k are listed in the sub-headings. Values of observed $|F|$ have been put on an absolute scale by dividing by the scale factor determined by least-squares refinement.

L	FC	FO	E
*** 0 0 L ***			
1	-22	16	1.0
2	243	258	5.2
4	152	155	3.2
5	-68	68	1.8
7	-67	66	1.8
8	101	99	2.3
9	-68	68	2.0
12	52	51	3.2
*** 0 2 L ***			
0	144	152	3.1
1	202	208	4.2
2	50	51	1.2
3	25	28	0.8
4	-22	21	0.5
6	-21	22	0.7
8	-28	27	1.0
9	-16	16	0.6
*** 0 4 L ***			
0	169	171	3.5
2	99	101	2.2
3	35	34	1.0
4	27	27	0.7
5	-37	37	1.1
7	-28	27	0.9
9	-36	36	1.0
*** 0 6 L ***			
0	338	327	6.6
1	-32	31	0.9
2	84	84	1.9
4	35	36	1.1
5	-48	47	1.4
6	-34	33	1.1
7	-43	40	1.4
8	50	52	1.5
12	30	31	2.3
*** 0 8 L ***			
1	117	116	2.5
3	34	32	1.0
6	-25	25	0.8
*** 0 10 L ***			
0	176	179	3.8
1	-39	38	1.1
2	110	108	2.4
4	63	60	1.7
5	-38	39	1.2
6	46	45	1.7
7	-41	42	1.8
8	22	23	1.3
9	-47	51	3.1
*** 0 12 L ***			
0	64	70	2.0
1	24	23	0.8
2	27	26	0.9
*** 0 14 L ***			
1	22	25	1.4
*** 0 16 L ***			
0	40	44	3.3
*** 1 15 L ***			
-6	-27	33	2.8
-4	-33	35	2.6
-3	20	21	1.5
-2	-31	31	2.1
-1	41	45	2.9
0	-34	34	2.1
1	53	57	3.6
3	50	52	3.7
5	43	47	3.8
6	-15	16	1.6
*** 1 13 L ***			
0	27	28	1.2
3	18	18	0.9
*** 1 11 L ***			
-9	27	27	1.9
-7	19	18	1.1
-5	29	29	0.9
-4	-37	37	1.2
-2	-42	41	1.3
-1	52	50	1.5
0	-40	40	1.3
1	64	64	1.8
2	24	24	0.7
3	44	43	1.3
5	33	32	1.3
*** 1 9 L ***			
-11	29	32	2.4
-9	40	43	2.3
-7	35	35	1.1
-5	18	19	0.7
-3	-27	28	0.9
-2	-14	14	0.7
-1	36	38	1.1
1	81	80	1.9
2	26	26	0.9
3	115	117	2.6
5	57	56	1.7
7	27	26	0.9
*** 1 7 L ***			
-12	29	34	2.7
-6	-35	36	1.0
-5	-39	38	1.3
-4	19	20	0.6
-3	-28	28	0.8
0	38	38	1.2
1	26	27	0.7
3	71	72	1.8
4	76	75	1.8
5	73	73	1.8
6	44	45	1.4
*** 1 5 L ***			
-13	52	56	4.6
-11	36	36	1.9
-9	65	65	1.9
-8	-40	41	1.4
-7	48	50	1.5
-6	-71	70	1.8
-5	58	59	1.6
-4	-133	131	2.8
-3	50	51	1.4
-2	-102	100	2.2
-1	216	210	4.3
0	-188	182	3.7
1	204	203	4.1
2	29	29	0.9
3	184	184	3.8
4	46	46	1.4
5	164	165	3.5
7	77	76	1.9
8	-55	55	1.7
9	42	44	1.4
10	-27	27	1.2
12	-35	38	2.7
*** 1 3 L ***			
-12	31	33	2.0
-11	21	21	1.2
-10	10	9	1.1
-9	42	43	1.4
-5	-26	27	0.8
-3	-235	231	4.7
-2	-31	30	1.0
-1	-32	33	1.0
0	50	52	1.2
1	24	26	0.7
2	44	50	1.2
3	295	289	5.8
4	64	64	1.6
5	32	32	1.0
6	30	30	0.9
9	-44	43	1.4
*** 1 1 L ***			
-13	44	45	3.3
-12	24	26	1.6
-11	50	50	2.2
-9	63	61	1.7
-7	30	29	1.0
-6	-27	27	0.9
-5	77	77	1.8
-4	42	39	1.2
-3	20	23	0.7
-2	-69	72	1.6
-1	136	144	2.9
0	-28	29	0.8
1	214	229	4.6
*** 1 1 L ***			
2	59	58	1.3
3	105	111	2.3
4	67	69	1.6
5	130	130	2.7
6	38	38	1.1
7	55	55	1.5
8	-27	26	1.1
10	-36	36	1.4
13	23	25	2.0
*** 2 0 L ***			
-12	49	49	3.0
-10	70	72	2.0
-8	158	155	3.3
-7	-21	20	0.8
-6	189	189	3.9
-5	-102	102	2.2
-4	261	258	5.2
-3	-102	107	2.3
-2	76	80	1.7
-1	-215	221	4.5
0	96	104	2.2
1	-150	157	3.2
2	114	118	2.5
3	-81	83	1.8
4	226	226	4.6
5	-34	34	0.9
6	227	227	4.6
8	136	136	2.9
10	42	42	1.7
12	33	34	2.3
*** 2 2 L ***			
-11	21	19	1.0
-10	62	61	2.0
-9	56	56	1.7
-8	41	40	1.4
-7	59	57	1.6
-6	18	19	0.6
-5	51	52	1.4
-4	-117	113	2.4
-3	26	25	0.8
-2	-23	23	0.7
-1	-14	15	0.5
0	-67	68	1.5
2	-46	44	1.2
3	-71	68	1.6
4	46	46	1.3
5	56	54	1.5
6	56	53	1.5
7	84	85	2.0
8	57	55	1.7
9	56	53	1.7
*** 2 4 L ***			
-10	54	54	2.1
-9	29	29	1.2
-8	77	75	1.9
-6	66	68	1.7
-3	-56	56	1.4
-2	55	53	1.4
-1	70	64	1.5
0	99	95	2.1
1	-69	69	1.6
3	-36	35	1.1
4	94	97	2.2
6	91	92	2.1
7	47	49	1.6
8	78	78	2.0
*** 2 6 L ***			
-12	26	27	2.1
-10	28	28	1.2
-8	84	86	2.1
-6	106	108	2.4
-5	-42	43	1.3
-4	81	80	1.9
-3	-44	43	1.3
-2	35	36	1.1
-1	-32	31	0.9
0	31	31	1.0
1	-41	43	1.3
3	-28	28	0.8
4	123	121	2.6
5	24	24	0.8
6	127	129	2.8
8	57	55	1.7
*** 2 8 L ***			
-10	34	36	2.2
-9	25	26	1.2
-8	23	23	0.9
*** 2 8 L ***			
-7	61	62	1.8
-5	47	46	1.4
-4	-56	56	1.6
-3	45	45	1.4
0	-39	39	1.1
1	26	25	0.9
4	35	36	1.3
5	65	67	1.8
6	36	36	1.0
7	45	45	1.4
8	19	18	0.8
9	41	42	2.2
*** 2 10 L ***			
-10	48	50	3.6
-8	67	68	3.5
-7	-26	28	1.1
-6	66	67	2.2
-5	-38	39	1.1
-4	59	58	1.7
-3	-69	68	1.9
-2	51	49	1.5
-1	-59	58	1.7
0	73	71	1.8
1	-81	80	2.0
2	50	50	1.6
3	-39	38	1.2
4	70	69	1.9
5	-38	38	1.2
6	76	74	2.6
8	74	77	4.2
10	26	25	2.1
*** 2 12 L ***			
-2	-15	16	0.7
-1	-27	27	1.0
0	-28	29	1.0
6	31	34	1.8
*** 2 14 L ***			
6	25	29	2.3
*** 2 16 L ***			
-3	-19	21	1.8
*** 3 15 L ***			
-5	42	45	3.8
-3	41	47	3.3
-1	38	40	2.8
1	27	29	2.1
2	-34	35	2.5
4	-31	33	2.6
*** 3 13 L ***			
-6	30	33	2.2
-4	25	25	1.4
*** 3 11 L ***			
-7	45	44	2.2
-6	-20	21	1.0
-5	49	50	1.8
-3	43	41	1.3
-1	17	18	0.6
0	-20	21	0.7
2	-38	38	1.1
3	21	21	0.9
5	26	25	1.2
7	39	39	2.4
9	34	35	2.7
*** 3 9 L ***			
-9	29	28	1.7
-7	31	31	1.1
-5	61	62	1.8
-4	28	28	0.9
-3	71	70	1.8
-1	66	66	1.7
2	-28	27	0.8
5	29	28	0.8
7	47	47	2.0
9	34	36	2.2
*** 3 7 L ***			
-8	34	30	1.2
-7	47	44	1.4
-6	74	71	1.9
-5	40	38	1.2
-4	43	42	1.4
*** 3 7 L ***			
-3	21	21	0.7
-1	23	23	0.7
0	23	23	0.6
1	-34	34	1.2
4	-45	43	1.3
7	20	20	0.6
10	37	40	2.7
11	31	34	2.6
*** 3 5 L ***			
-12	-33	33	2.3
-11	27	27	1.5
-9	53	55	1.7
-8	-25	25	0.7
-7	146	146	3.2
-5	175	174	3.6
-3	127	127	2.7
-2	-19	19	0.5
-1	95	95	2.1
0	-36	37	1.2
1	87	87	2.0
2	-122	121	2.6
3	50	50	1.4
4	-98	98	2.2
5	68	68	1.8
6	-69	71	1.8
7	84	83	2.1
8	-30	30	0.8
9	58	58	2.2
11	57	59	4.0
*** 3 3 L ***			
-9	22	22	0.8
-8	54	54	1.6
-7	-22	21	0.6
-6	81	80	2.0
-5	86	86	2.0
-4	120	118	2.5
-3	57	59	1.5
-2	-83	79	1.8
-1	142	137	2.8
0	36	37	0.9
1	-205	203	4.1
2	-65	63	1.5
3	-23	24	0.8
7	58	56	1.6
8	44	42	1.3
10	39	39	1.8
*** 3 1 L ***			
-12	-33	31	1.9
-9	51	51	1.6
-7	115	115	2.5
-6	27	29	1.0
-5	103	103	2.3
-3	106	108	2.3
-2	41	37	1.1
-1	37	40	1.1
1	22	23	0.8
2	35	33	1.0
3	95	94	2.1
4	-42	42	1.2
5	40	42	1.3
6	-39	39	1.2
7	80	79	2.0
9	66	66	1.9
10	34	36	1.7
11	56	55	3.2
*** 4 0 L ***			
-11	-65	66	3.1
-10	44	42	1.7
-9	-53	55	1.7
-8	70	70	1.9
-7	-93	91	2.1
-6	107	106	2.4
-5	-11	12	0.7
-4	96	99	2.2
-2	406	394	7.9
-1	175	169	3.5
0	239	243	4.9
1	-148	146	3.0
2	222	223	4.5
3	-20	20	0.7
4	30	30	0.9
5	-96	97	2.2
6	102	101	2.3
7	-72	72	1.9
8	50	50	1.7
9	-59	58	2.1
10	68	68	3.2
12	31	31	2.3
*** 4 2 L ***			
-8	-25	26	0.7
-7	24	26	0.9
-5	42	43	1.4
-4	43	44	1.3
-3	57	57	1.5
-2	179	177	3.6
-1	88	89	1.9
1	105	104	2.2
2	-53	50	1.4
3	21	21	0.7
7	-22	23	0.7
8	-32	32	0.8
*** 4 4 L ***			
-11	-30	30	1.7
-9	-31	33	1.0
-7	-31	32	1.1
-6	38	37	1.2
-5	29	29	0.9
-4	99	98	2.2
-2	105	104	2.3
-1	22	23	0.8
0	59	61	1.5
2	18	19	0.6
3	-20	21	0.6
4	19	19	0.6
5	-32	30	1.1
6	30	30	0.8
7	-45	44	1.5
*** 4 6 L ***			
-11	-28	27	1.7
-10	34	33	1.7
-9	-36	34	1.3
-7	-53	52	1.7
-6	47	46	1.4
-4	45	45	1.3
-2	141	139	3.0
-1	48	49	1.4
0	88	89	2.0
1	-42	41	1.2
2	74	74	1.8
3	-37	38	1.2
4	-25	24	0.8
5	-65	65	1.7
6	46	46	1.4
7	-30	30	0.9
8	32	32	1.3
9	-31	30	1.5
10	38	37	2.4
*** 4 8 L ***			
-5	34	34	0.9
-3	40	39	1.3
-2	89	89	2.1
-1	57	57	1.7
1	77	75	1.9
2	-23	22	0.8
3	14	14	0.7
4	-19	19	0.6
8	-22	23	1.2
*** 4 10 L ***			
-9	-35	36	2.3
-8	38	38	2.1
-7	-41	42	2.1
-6	51	50	1.9
-4	82	82	2.1
-2	95	96	2.3
0	87	87	2.1
1	-37	37	1.1
2	68	68	1.9
3	-28	28	0.8
4	54	53	1.7
5	-38	38	1.4
6	35	38	1.8
7	-55	59	3.2
9	-28	29	2.3
*** 4 12 L ***			
-3	21	21	1.0
-2	43	47	1.9
-1	26	27	1.1
0	20	21	0.8
*** 4 14 L ***			
-2	38	36	2.5
*** 4 16 L ***			
-2	19	21	1.9
*** 4 16 L ***			
0	20	24	2.1
*** 5 15 L ***			
-4	-25	27	2.3
-3	26	30	2.5
-1	31	34	2.6
1	42	47	3.7
3	38	41	3.5
*** 5 13 L ***			
2	27	28	1.6
*** 5 11 L ***			
-4	-27	27	1.1
-3	34	33	1.3
-1	42	40	1.5
1	59	59	2.0
3	31	30	1.4
5	31	31	1.7
*** 5 9 L ***			
-7	21	21	1.0
-6	-26	27	1.0
-4	-27	28	0.9
-3	35	36	1.1
-1	53	52	1.5
0	30	30	0.9
1	70	67	1.8
2	26	25	0.9
3	50	51	1.6
5	30	31	1.1
8	-21	22	1.5
*** 5 7 L ***			
-8	-23	22	1.0
-7	-31	32	0.9
-3	17	17	0.7
-2	26	26	0.8
-1	43	43	1.5
0	34	34	1.2
2	68	65	1.8
3	48	48	1.4
4	36	35	0.9
*** 5 5 L ***			
-11	55	59	3.6
-9	32	32	1.2
-8	-61	59	1.9
-7	32	31	0.8
-6	-71	71	1.9
-4	-63	61	1.7
-3	114	113	2.5
-2	-47	48	1.4
-1	94	95	2.2
1	187	186	3.8
3	114	113	2.5
5	78	77	2.0
6	-49	50	1.5
7	54	53	1.7
8	-35	35	1.4
9	31	32	1.8
10	-41	43	2.9
*** 5 3 L ***			
-12	29	31	2.1
-6	-31	32	1.0
-5	-45	45	1.4
-4	-40	42	1.4
-2	15	15	0.6
-1	24	24	0.7
0	79	79	1.8
1	83	85	2.0
2	112	110	2.4
3	47	47	1.5
7	-37	39	1.2
*** 5 1 L ***			
-13	34	35	2.7
-11	47	48	2.4
-9	28	28	1.1
-8	-43	43	1.3
-7	34	34	1.0
-5	17	17	0.7
-4	-41	42	1.2
-3	90	88	2.0
-2	42	42	1.3
-1	140	143	3.0
0	39	38	1.1
1	108	112	2.4
*** 5 1 L ***			
2	21	22	0.6
3	83	88	2.0
4	35	35	1.1
5	58	56	1.6
7	25	25	0.7
8	-40	41	1.2
10	-32	32	1.7
*** 6 0 L ***			
-12	52	53	3.7
-10	77	74	3.2
-9	30	32	1.1
-8	74	75	2.0
-7	-26	26	0.7
-6	107	108	2.5
-5	-56	58	1.6
-4	83	88	2.0
-3	-164	162	3.5
-2	57	60	1.6
-1	-37	38	1.2
0	62	62	1.8
1	-101	103	2.3
2	163	165	3.5
4	156	161	3.4
6	121	121	2.7
8	37	36	1.4
10	35	37	2.3
*** 6 2 L ***			
-11	46	48	2.8
-10	36	35	1.6
-9	27	26	0.9
-8	45	45	1.5
-7	22	22	0.7
-5	-30	29	1.0
-4	-33	34	1.0
-2	-35	36	1.0
1	23	23	0.7
3	54	55	1.6
4	35	37	0.9
5	67	66	1.8
6	35	35	1.0
7	48	50	1.4
*** 6 4 L ***			
-10	47	48	2.4
-8	54	57	1.7
-5	-65	64	1.8
-3	-18	18	0.6
-2	48	49	1.5
-1	-21	21	0.7
0	18	18	0.8
2	80	83	2.0
4	62	61	1.8
5	30	30	1.0
6	60	57	1.7
11	-22	25	2.2
*** 6 6 L ***			
-10	44	43	2.6
-8	46	44	1.8
-6	40	38	1.2
-5	-44	43	1.4
-4	44	44	1.4
-3	-63	63	1.8
-2	36	36	1.0
1	-38	37	1.1
2	96	95	2.3
3	23	23	0.7
4	102	105	2.5
6	55	54	1.8
*** 6 8 L ***			
-8	32	33	1.7
-2	-26	26	0.9
1	27	27	0.8
3	59	59	1.8
4	28	27	0.9
5	41	42	1.5
7	37	34	1.8
*** 6 10 L ***			
-10	40	43	3.6
-8	38	39	2.5
-6	37	36	1.8
-5	-45	46	2.0
-4	32	31	1.1
-3	-56	53	2.1
-2	37	37	1.2
-1	-39	40	1.4
0	41	40	1.2
*** 6 10 L ***			
1	-40	38	1.3
2	66	64	2.3
3	-31	31	1.2
4	52	51	2.3
6	56	59	3.7
8	26	76	2.1
*** 7 11 L ***			
-5	43	43	2.6
-3	30	30	1.5
-2	-24	25	1.3
0	-33	34	1.8
2	-31	31	1.6
3	27	29	1.7
*** 7 9 L ***			
-7	35	34	1.9
-5	45	49	2.1
-3	40	40	1.3
0	-33	33	1.0
5	35	36	1.9
7	34	36	2.5
*** 7 7 L ***			
-8	35	35	1.9
-7	33	33	1.5
-6	35	37	1.3
-5	33	33	1.1
-4	11	12	1.0
1	-20	19	0.7
8	23	26	1.8
*** 7 5 L ***			
-11	26	26	2.0
-9	39	38	.9
-8	25	24	1.2
-7	85	85	2.4
-5	101	101	2.4
-4	-41	41	1.3
-3	93	94	2.2
-2	-34	33	1.1
-1	25	26	0.8
0	-72	74	1.9
1	47	47	1.5
2	-93	93	2.2
3	66	66	1.9
4	-40	39	1.2
5	56	57	1.8
7	28	27	1.2
9	46	46	3.2
*** 7 3 L ***			
-9	21	20	1.1
-7	36	36	1.1
-6	73	73	2.0
-5	40	41	1.3
-3	36	36	1.1
-2	21	22	0.6
-1	-37	37	1.3
0	-67	68	1.8
1	-59	59	1.7
2	36	36	1.0
3	-36	36	1.1
5	38	39	1.1
6	37	39	1.3
7	26	25	1.0
*** 7 1 L ***			
-9	37	37	1.5
-8	27	27	0.8
-7	65	68	2.0
-5	98	100	2.4
-3	58	60	1.7
-2	-41	42	1.4
0	-28	28	1.0
1	54	57	1.6
2	-39	38	1.4
3	46	49	1.4
4	-22	21	0.8
5	57	58	1.8
6	26	26	0.7
7	42	43	1.7
9	47	48	2.8
11	22	23	2.1
*** 8 0 L ***			
-6	63	62	1.9
-5	-22	23	0.8
-4	155	156	3.4
-3	46	47	1.5
*** 8 0 L ***			
-2	149	152	3.3
-1	-34	36	1.2
0	108	108	2.5
1	-44	44	1.5
2	76	76	2.0
3	-81	84	2.2
4	30	30	1.0
8	47	49	2.8
10	41	43	3.5
*** 8 2 L ***			
-7	26	27	0.9
-5	34	34	1.1
-4	70	73	1.9
-3	72	74	1.9
-2	42	44	1.3
-1	30	30	0.9
2	-32	33	1.1
5	-20	22	0.8
*** 8 4 L ***			
-6	45	44	1.4
-4	71	70	1.9
-3	17	16	0.8
-2	69	67	1.9
0	26	26	0.8
1	-31	32	0.9
3	-39	40	1.2
4	16	16	0.7
*** 8 6 L ***			
-6	40	38	1.4
-4	73	75	2.0
-2	76	74	2.0
0	54	52	1.7
1	-40	41	1.2
3	-59	58	1.9
*** 8 8 L ***			
-7	21	23	1.6
-5	28	26	1.3
-4	34	33	1.3
-3	48	48	1.7
-1	29	28	1.0
2	-28	27	1.0
*** 8 10 L ***			
-6	42	43	2.8
-4	63	62	3.5
-2	59	59	2.9
0	39	40	2.1
1	-30	28	1.5
2	45	44	2.4
*** 9 11 L ***			
-3	30	33	2.6
-1	35	36	2.5
*** 9 9 L ***			
-1	39	40	2.0
1	45	45	2.4
3	33	33	2.1
*** 9 7 L ***			
-1	25	24	1.0
0	27	26	1.1
1	37	38	1.4
*** 9 5 L ***			
-10	-31	35	2.7
-6	-18	36	1.5
-5	43	43	1.7
-4	-28	28	1.0
-3	52	51	1.5
-2	-28	28	0.8
-1	86	86	2.2
1	77	74	2.2
3	53	53	2.0
*** 9 3 L ***			
-2	42	43	1.3
-1	40	39	1.0
0	38	39	1.2
1	52	52	1.5
3	28	28	1.0
*** 9 1 L ***			
-5	29	29	0.8
-3	68	70	2.0
-1	73	72	2.0
1	70	74	2.0
3	47	44	1.5
8	-29	31	2.1
*** 10 0 L ***			
-10	44	49	3.7
-8	33	32	2.0
-7	-24	22	1.2
-6	39	39	1.7
-5	-56	55	2.0
-4	33	31	1.2
-3	-25	25	0.8
-2	41	41	1.1
-1	-33	32	1.0
2	74	73	2.5
4	79	75	3.4
6	43	40	2.6
*** 10 2 L ***			
0	23	22	0.8
2	32	31	1.3
5	33	33	1.8
*** 10 4 L ***			
0	40	39	1.3
2	50	49	1.9
4	41	40	2.1
*** 10 6 L ***			
0	25	24	1.1
2	55	53	2.7
4	45	46	2.7
6	28	30	2.3
*** 10 8 L ***			
2	25	25	1.6
*** 10 10 L ***			
2	33	33	2.7
*** 11 5 L ***			
-9	40	45	4.0
-7	40	42	3.1
-5	39	42	2.6
3	44	45	2.8
*** 11 3 L ***			
-7	25	27	1.8
*** 11 1 L ***			
-9	33	36	3.0
-7	43	44	2.9
1	20	19	1.2
3	37	37	2.1
5	35	34	2.3
7	33	34	2.9
*** 12 0 L ***			
-6	53	53	3.6
-4	51	51	3.0
-2	31	31	1.7
1	-30	29	1.8
*** 12 4 L ***			
-6	35	35	2.7
*** 13 5 L ***			
-3	36	38	3.1
-1	41	41	3.2
*** 13 1 L ***			
-3	36	39	2.7
-1	37	37	2.6
1	22	21	1.7

Structure solution and refinement

A three-dimensional gradient-sharpened (Jacobson, Wunderlich & Lipscomb, 1961) Patterson function in which the coefficients were

$$E_{\text{hl}}^2[1+6(\sin\theta/\lambda)^2]\exp[-4{\cdot}72(\sin\theta/\lambda)^2]$$

was calculated. Inspection of the diagram revealed prominent well-defined peaks, all of which were accounted for in space group $C2/m$ as metal–metal interactions. Iron atoms were assigned to two non-equivalent equipoints of point symmetry $2/m$, $2(a)$ (000) and $2(d)$ $(0\frac{1}{2}\frac{1}{2})$. Manganese atoms were assigned to two non-equivalent equipoints, $4(i)$ $(x0z)$, point symmetry m, and $4(h)$ $(0y\frac{1}{2})$, point symmetry 2. An electron-density map, phased from the metal-atom positions, and weighted with the function (Woolfson, 1956)

$$\tanh[|F_{\text{obs}}|\,.\,|F_{\text{calc}}|/\Sigma\,(f_{\text{C}}^2+f_{\text{O}}^2)\exp(-10{\cdot}6\sin^2\theta/\lambda^2)]$$

revealed peaks corresponding to all the carbon and oxygen atoms in the asymmetric unit: one C and one O in $4(g)$ $(0y0)$; one C and one O in $4(h)$ $(0y\frac{1}{2})$; four C and four O in $4(i)$ $(x0z)$; and four C and four O in $8(j)$ (xyz).

The structure was refined by the full-matrix least-squares method, in which $\Sigma w(F_o^2-S^2F_c^2)^2$ was minimized. The parameters refined were 47 positional parameters, 112 coefficients of the anisotropic temperature factors, and one scale factor S. The measures of agreement achieved are $R_F=2{\cdot}47\%$, $R_{F^2}=4{\cdot}41\%$, and $\sigma_1\equiv[\Sigma w(F_{\text{obs}}^2-S^2F_{\text{calc}}^2)^2/(m-n)]^{\frac{1}{2}}=1{\cdot}12$ for $m-n=642$ degrees of freedom. The observed and calculated values of F^2 are listed in Table 1; the final parameters are in Table 2.

Results and discussion

The arrangement of molecules in the structure is best understood by reference to Fig. 4, which shows the metal atoms alone. The linear triatomic groups have two distinct orientations – one lying in the mirror planes of symmetry across twofold rotation axes, and the other along twofold rotation axes across mirror planes. One molecule of each type is shown in Fig. 5. Both conform to the symmetry of point group $2/m$, but with the symmetry elements differently disposed.

Fig. 5 also lists the interatomic distances and bond angles within each molecule. The least-squares standard errors are about 0·003 Å for Fe–Mn bonds and 0·01 Å for others, 0·2° for Mn–Fe–Mn angles, 0·3° for M–M–C angles, and 0·6° for M–C–O angles. In spite of the difference in orientation of symmetry elements, the similarity of the two molecules is striking. The greatest discrepancy, 0·03 Å in the Fe–Mn bond distances, is examined in detail below; the mean value of this distance, 2·815 Å, compares well with the average of the Mn–Mn bond, 2·923 Å, in $Mn_2(CO)_{10}$ and the non-bridged Fe–Fe bonds, 2·685 Å, in $Fe_3(CO)_{12}$ (Wei & Dahl, 1966). The average Fe–C bond distance is 1·792 Å, in good agreement with previously determined values. The Mn–C bond lengths fall into two groups: those normal to the metal–metal axes (equatorial) average 1·855 Å; those along these axes (apical)

Table 2. *Parameters of the structure of* $Mn_2Fe(CO)_{14}$

The elements β_{ij} form the matrix $\boldsymbol{\beta}$ in the temperature factor exp $(-\mathbf{h}^T\boldsymbol{\beta}\mathbf{h})$, where $\mathbf{h}$ is the Miller index triple. Least-squares standard errors are indicated in parentheses.

	Fractional coordinates ×10⁴			Temperature factor matrix elements $\beta_{ij}\times10^4$					
	x	*y*	*z*	11	22	33	12	13	23
Fe(1)	0	0	0	71 (1)	66 (1)	60 (1)	0	12 (1)	0
C(1, 1)	580 (6)	0	1486 (7)	75 (7)	95 (6)	82 (8)	0	14 (6)	0
O(1, 1)	946 (5)	0	2441 (5)	115 (6)	165 (6)	84 (6)	0	−1 (5)	0
C(1, 2)	0	1250 (7)	0	95 (8)	94 (7)	92 (8)	0	21 (6)	0
O(1, 2)	0	2062 (5)	0	183 (8)	70 (4)	175 (8)	0	44 (6)	0
Mn(1)	2200 (1)	0	−653 (1)	70 (1)	57 (1)	51 (1)	0	7 (1)	0
C(1, 3)	1693 (4)	912 (4)	−1717 (4)	82 (5)	71 (4)	77 (5)	−5 (3)	11 (4)	−2 (4)
O(1, 3)	1401 (3)	1465 (3)	−2377 (3)	151 (4)	85 (3)	113 (5)	6 (3)	9 (3)	42 (3)
C(1, 4)	3610 (7)	0	−1042 (6)	87 (8)	88 (6)	81 (7)	0	12 (6)	0
O(1, 4)	4498 (5)	0	−1288 (5)	84 (5)	152 (6)	123 (6)	0	29 (5)	0
C(1, 5)	2525 (4)	940 (4)	432 (4)	94 (5)	67 (3)	77 (5)	−4 (3)	4 (4)	13 (3)
O(1, 5)	2749 (4)	1537 (3)	1055 (4)	175 (5)	75 (3)	106 (4)	−22 (3)	−6 (3)	−21 (3)
Fe(2)	0	5000	5000	54 (1)	33 (1)	48 (1)	0	7 (1)	0
C(2, 1)	1282 (6)	5000	4358 (5)	75 (7)	60 (4)	59 (6)	0	5 (5)	0
O(2, 1)	2106 (5)	5000	3948 (5)	91 (5)	109 (4)	113 (6)	0	45 (4)	0
C(2, 2)	819 (5)	5000	6408 (6)	63 (6)	43 (4)	83 (7)	0	28 (5)	0
O(2, 2)	1353 (4)	5000	7283 (4)	96 (5)	98 (4)	63 (4)	0	−17 (4)	0
Mn(2)	0	3041 (1)	5000	76 (1)	35 (1)	68 (1)	0	5 (1)	0
C(2, 3)	0	1772 (6)	5000	145 (9)	57 (5)	98 (8)	0	−2 (7)	0
O(2, 3)	0	982 (4)	5000	309 (12)	30 (3)	215 (9)	0	−10 (8)	0
C(2, 4)	1490 (5)	3152 (3)	5650 (4)	91 (6)	44 (3)	80 (5)	14 (3)	7 (4)	−3 (3)
O(2, 4)	2402 (4)	3210 (3)	6055 (3)	83 (3)	88 (3)	135 (4)	24 (3)	−14 (3)	−16 (3)
C(2, 5)	437 (4)	3088 (3)	3538 (5)	85 (5)	49 (3)	95 (6)	6 (3)	1 (4)	−3 (3)
O(2,5)	700 (3)	3096 (3)	2635 (3)	148 (5)	99 (3)	78 (4)	11 (3)	30 (3)	−5 (3)

average 1·805 Å. These bond lengths are close to the corresponding values in $Mn_2(CO)_{10}$, 1·830 and 1·792 Å.

The environment of each metal atom is nearly octahedral; however, around each Mn atom, the equatorial C–O groups are appreciably displaced toward the center of the molecule, resulting in an average Fe–Mn–bond angle of 86·6°. A similar departure from 90° was observed in $Mn_2(CO)_{10}$ and $Tc_2(CO)_{10}$, in which the effect was attributed to repulsion between the apical and equatorial carbon atoms.

The C–O bond lengths average 1·14 Å with no appreciable variation with position in the molecule. The M–C–O angles range between 176·6° and 180·0°, averaging 179·1°.

The conformation of both molecules about the Fe–Mn bond axis results in the staggered configuration of equatorial ligands shown in Fig. 6, again similar to the conformation in $Mn_2(CO)_{14}$.

The root-mean-square thermal displacements of the atoms are indicated by the ellipsoids in the drawings of the structure. These displacements suggest either rigid-body oscillations or bending of metal–carbon bonds or both. A calculation of the rigid-body amplitudes according to Cruickshank's (1956) analysis did not yield a satisfactory fit to the observed displacements, indicating that bending motions are also appreciable.

Because the interatomic distances given in Fig. 5 are uncorrected for the effects of thermal motion, they must be shorter than the true mean bond lengths (Busing & Levy, 1964). The amount of shortening cannot be reliably estimated in the absence of a specific model for the thermal motion of the molecules. However, the riding model (Busing & Levy, 1964) should in this case provide an upper limit to the corrections for the metal–metal and metal–carbon links; these are 0·000 and 0·006 Å for the former and range from 0·004 to 0·020 Å for the latter, averaging 0·008 Å. The effects thus appear to be no larger than the experimental errors.

We now examine the significance of the difference of 0·03 Å between the two Fe–Mn bond lengths found in the structure and ask whether the hypothesis that the two bond lengths are equal can be rejected, on the basis of the data, at some reasonable level of confidence. Accordingly, an alternate least-squares refinement of the structure was made, in which the y parameter of Mn(2) was constrained as a function of the parameters of Mn(1) to a value making the distances equal. The weighted quadratic residual sum for this refinement is $R_H = 1374$, compared to $R_0 = 800$ for the non-constrained refinement. Hamilton (1964) shows that the hypothesis may be tested by examining the quantity $Q = (R_H - R_0)/R_0$, which is distributed as

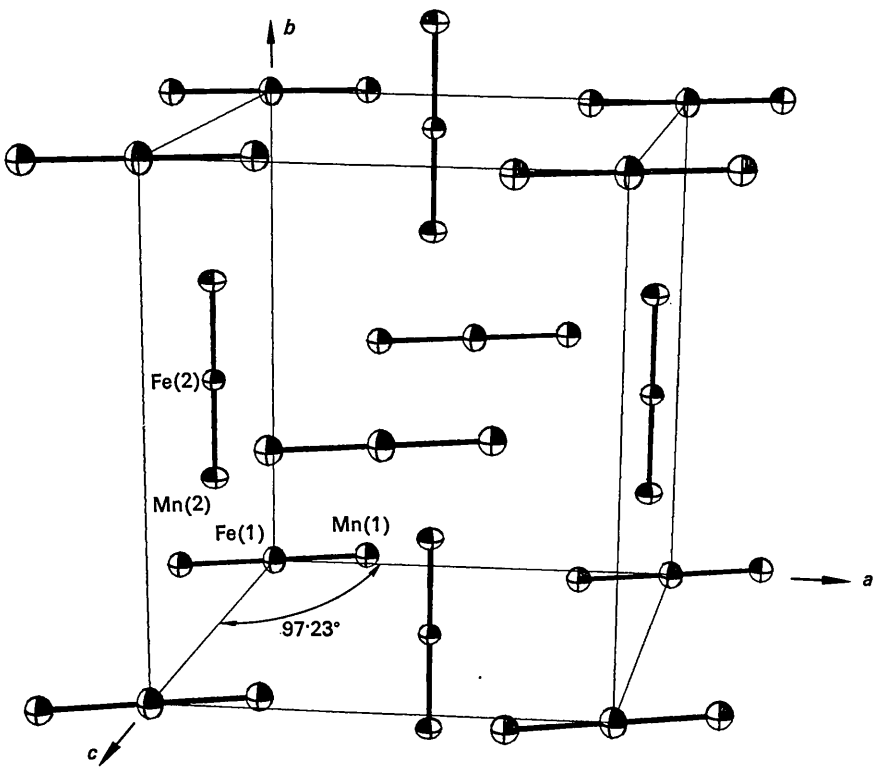

Fig. 4. The arrangement of Fe and Mn atoms in the unit cell of $Mn_2Fe(CO)_{14}$. The atoms are represented by ellipsoids for which the major axes are 1·54 of the r.m.s. principal thermal displacements; at this scale, the surface encloses 50% of normally distributed displacements (Johnson, 1965).

$(b/m-n)F_{b,m-n}$, where $b=1$ is the rank of the hypothesis, $m-n=642$ is the number of degrees of freedom in the non-constrained refinement, and $F_{b,m-n}$ is the variance-ratio function, for which the distribution is known and critical percentage points are tabulated. In the present case, $Q=0{\cdot}718$ is much greater than $(F_{1,642,0{\cdot}005})/642=0{\cdot}0123$, the value of $(F_{1,642})/642$ for 99·5% confidence level. Thus the hypothesis can be rejected at a confidence level much higher than 99·5%.

This conclusion, of course, is based entirely on the fit of the model to the particular set of data collected in this study. It might be invalidated by the presence of systematic errors in the data, and we must raise the question of whether such errors could arise from faulty integration of the reflections in the stationary-crystal procedure, or from the rejection from consideration of all the weak reflections. Since the chemical structure is the same in both molecules, and since there are no

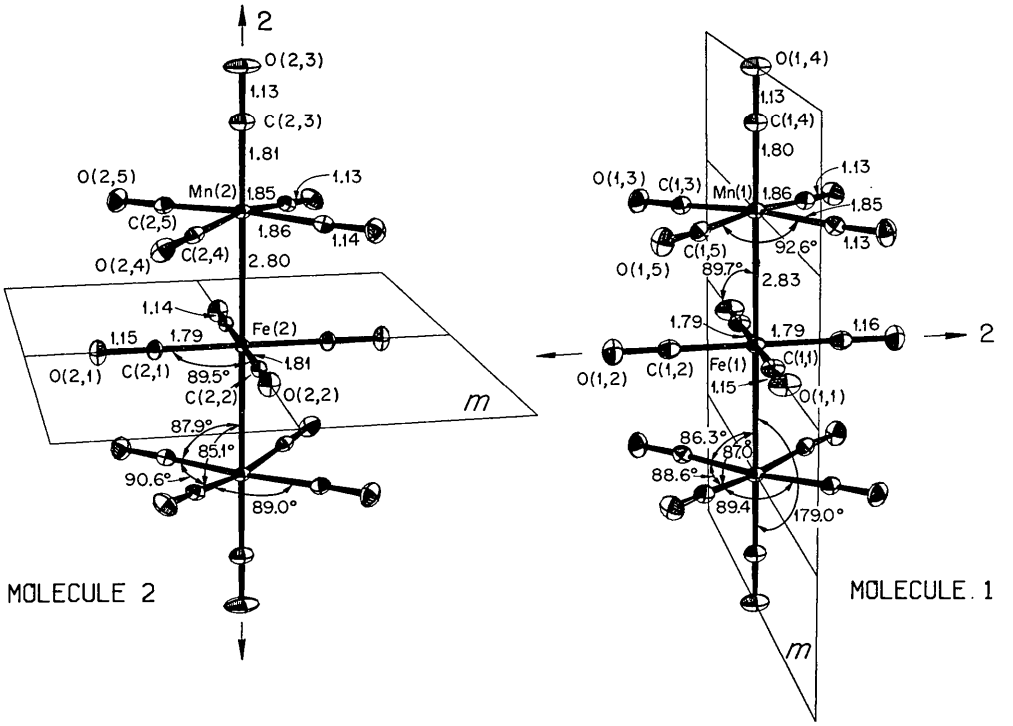

Fig. 5. The molecule of $Mn_2Fe(CO)_{14}$ as it occurs in two non-equivalent positions in the crystal. The atoms are represented by 10% probability ellipsoids (major axes 0·77 of the r.m.s. principal displacements).

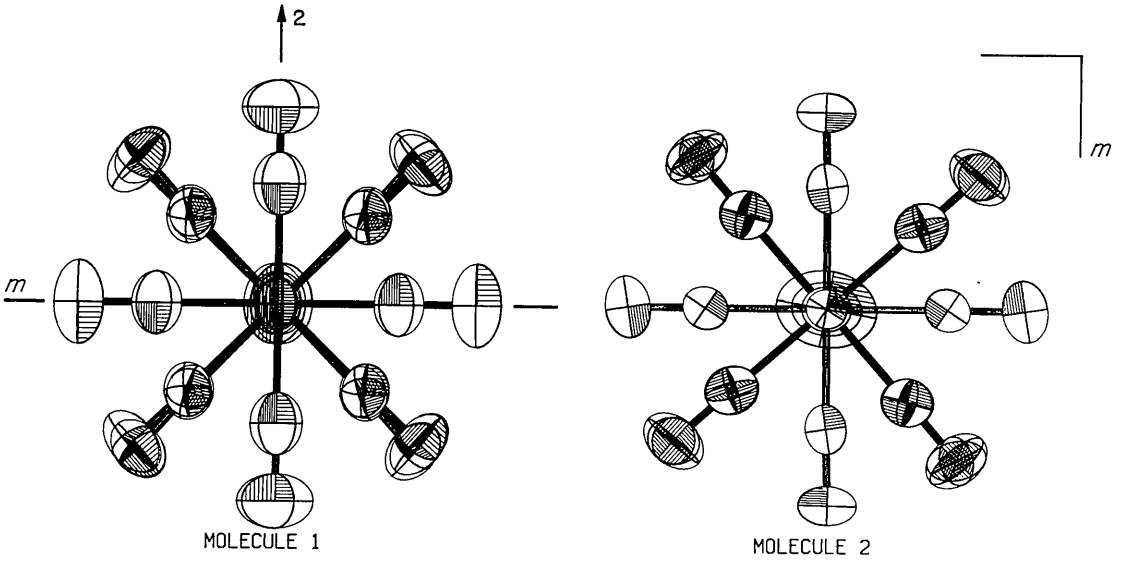

Fig. 6. The two molecules viewed along the metal–metal axis, showing the conformation of the equatorial carbonyl groups. The ellipsoids are for 50% probability.

pronounced intermolecular interactions, a real difference in bond length is not plausible. Consequently the question of systematic error in the data set demands further study.

Computations for this work were carried out on an IBM 360/75 and a CDC 1604 electronic computer. Programs used, with accession numbers in the *World List of Crystallographic Computer Programs* (Shoemaker, 1966), are as follows:

Absorption correction	(*a*)	523
Statistical analysis of data	ORSTAT	496
Fourier synthesis	XFOUR(*b*)	391
Least-squares refinement	XFLS	389
Distances and angles	ORFFE(*c*)	363
Structure drawings	ORTEP	387
Rigid-body analysis	UCLATO1	232
Structure factor table	EDIT	393

(*a*) Modified for the CDC 1604 and generalized to a general ellipsoid by C.K.Johnson of this Laboratory.
(*b*) Modified for the IBM 360/75 by G.Brunton of this Laboratory.
(*c*) Modified for the IBM 360/75 by C.K.Johnson.

The authors are indebted to Professor R.K.Sheline of Florida State University, who kindly furnished the material for this study.

References

BAILEY, M. F. & DAHL. L. F. (1965). *Inorg. Chem.* **4**, no.8, 1140.
BUSING, W. R. & LEVY, H. A. (1964). *Acta Cryst.* **17**, 142.
BUSING, W. R., ELLISON, R. D., LEVY, H. A., KING, S. P. & ROSEBERRY, R. T. (1967). Report ORNL-4143, Oak Ridge National Laboratory, Oak Ridge, Tenn., U.S.A.
CRUICKSHANK, D. W. J. (1956). *Acta Cryst.* **9**, 754.
DAHL, L. F. & RUNDLE, R. E. (1963). *Acta Cryst.* **16**, 419.
EVANS, G., HARGADEN, J. P. & SHELINE, R. K. (1967). Florida State Univ., Tallahassee, Fla., U.S.A., Private communication.
HAMILTON, W. C. (1964). *Statistics in Physical Science*, p.139. New York: Ronald Press Co.
JACOBSON, R. A., WUNDERLICH, J. A. & LIPSCOMB, W. N. (1961). *Acta Cryst.* **14**, 598.
JOHNSON, C. K. (1965). Report ORNL-3794, Revised, Oak Ridge National Laboratory, Oak Ridge, Tenn., U.S.A., page 70.
MACK, M. & SPIELBERG, N. (1958). *Spectrochim. Acta*, **12**, 169.
POWELL, H. M. & EWENS, R. V. G. (1939). *J. Chem. Soc.* p.286.
SCHUBERT, E. H. & SHELINE, R. K. (1965). *Z. Naturforsch.* **20b**, 1306.
SHOEMAKER, D. P. (1966). *World List of Crystallographic Computer Programs*, 2nd edition. Utrecht: Oosthoek.
WEI, C. H. & DAHL, L. F. (1966). *J. Amer. Chem. Soc.* **88**, 1821.
WOOLFSON, M. M. (1956). *Acta Cryst.* **9**, 804.

Acta Cryst. (1967). **23**, 1086

X-Ray Structure Analysis of Deca-*trans*-3, *trans*-7-dienedioic Acid

BY E. MARTUSCELLI

Sezione VII, *Centro Nazionale di Chimica delle Macromolecole, C.N.R., c/o Istituto Chimico, Via Mezzocannone* 4, *Napoli, Italy*

(*Received* 17 *July* 1967)

The crystal structure of deca-*trans*-3, *trans*-7-diene-1,10-dioic acid, $C_{10}H_{14}O_4$, has been determined by three-dimensional X-ray diffraction analysis. The compound crystallizes in the centrosymmetric monoclinic space group $C2/c$. The unit cell contains four molecules and has the dimensions $a=21{\cdot}74\pm0{\cdot}02$, $b=4{\cdot}66\pm0{\cdot}01$, $c=10{\cdot}40\pm0{\cdot}01$ Å; $\beta=106°\pm30'$. A trial structure was obtained by examination of the Patterson projections on the (010), (001) and (100) planes. The atomic parameters were refined by the differential synthesis method. The molecules are associated in rows in the crystal lattice. The rows in successive planes parallel to $(\bar{2}01)$ are oblique to one another. Noteworthy characteristics are the internal rotation angles about the single bonds C(2)–C(3) (−125·5°) and C(4)–C(5) (−1·6°).

Introduction

The three-dimensional study of the crystal and molecular structure of deca-*trans*-3, *trans*-7-diene-1,10-dioic acid is part of a research program whose main goal is the determination of the conformational parameters that a number of important atomic groups (generally of aliphatic nature) assume in the crystal state. In the present case we are interested in determining the conformation of the group

$$(\text{–C–CH}_2\text{–CH=CH–CH}_2\text{–CH}_2\text{–CH=CH–CH}_2\text{–C–})$$

comprised between the two acidic functional groups of the molecule, and particularly the values of the